

MODEL OF STRUCTURAL FRAGMENTATION INDUCED BY HIGH PRESSURE TORSION

Jan Kratochvíl¹, Martin Kružík² and Radan Sedláček³

¹Czech Technical University, Faculty of Civil Engineering, Department of Physics, Thákurova 7, 166 29 Prague, Czech Republic and Charles University, Faculty of Mathematics and Physics, Mathematical Institute, Sokolovská 83, 186 75 Prague, Czech Republic

²Institute of Information Theory and Automation of the ASCR, Pod vodárenskou věží 4, 182 08 Prague, Czech Republic and Czech Technical University, Faculty of Civil Engineering, Department of Physics, Thákurova 7, 166 29 Prague, Czech Republic

³Technische Universität München, Fakultät für Maschinenwesen Lehrstuhl für Werkstoffkunde und Werkstoffmechanik Boltzmannstr. 15, 85747 Garching, Germany

Received: November 11, 2009

Abstract. The paper analyzes mechanisms of ultra-fine grain substructure formation as observed in high pressure torsion (HPT) experiments. Accepting that HPT shearing is achieved by intergranular glide (M. Hafok and R. Pippa, *Scripta Materialia*, 56:757-760, 2007) the fragmentation process is interpreted within the framework of crystal plasticity. The deformation is treated as a plastic flow though the adjustable crystal lattice fragmented into misoriented regions. The basic feature of the substructure formation is an effective rotation of the slip systems approaching asymptotically the observed steady state. The fragmentation is interpreted as an instability of the homogeneous deformation mode. It is proposed that the rotation causes a continuous reconstruction of the substructure pattern. The hindered destruction of the previous pattern leads to enhanced hardening. The size of the structural elements seems to result from the competition between two tendencies: the internal and dissipative energy tend to decrease the structural size, whereas the short-range dislocation interactions oppose this tendency.

1. INTRODUCTION

High-pressure torsion (HPT) is highly suitable for experimental and theoretical studies of formation of the ultra-fine grain substructure: very high strain can be achieved without interruption, one can look at various amount of strain in one specimen, due to relatively simple loading conditions strain can be defined approximately as simple shear. It is only within approximately 5 years that numerous extensive reports documenting the processing and properties of materials fabricated by HPT have started

appearing in the scientific literature. The large number of recent publications reviewed recently in [1-4] indicates that the research is still mostly empirical. It is striking that there are only very few attempts to understand the mechanisms of ultra-fine grain substructure formation.

Most of the approaches are based on the idea that heavy straining introduces in the deformed material very high dislocation density and that the dislocations arrange themselves into an ultra-fine substructure assisted by dynamic recovery [5-10]. The

Corresponding author: Jan Kratochvil, e-mail: kratochvil@fsv.cvut.cz

most advanced version of this approach was suggested by Alexandrov *et al.* [9] and Estrin *et al.* [10]. The material is considered in the form of a two-phase composite. The separate phases correspond to the dislocation cells boundaries where dynamic recovery occurs by climb processes and the cell interiors where dynamic recovery is controlled by the annihilation of dislocations by cross-slip. In [9] the upgraded Estrin-Tóth dislocation model has been presented to describe the experimental data observed on Cu. It is an attempt to analyze thoroughly the microstructure evolution of pure metals subjected to severe plastic deformation. In [10] the strain gradient plasticity model uses a conventional relationship for the change in dislocation density within the cell interiors and cell boundaries due to activation of Frank-Read sources. The basic assumption of a complementary modelling reported in [11] is that the lattice rotation is impeded in grain mostly near grain boundaries. This is the reason for lattice curvatures that appear during large plastic strain. The curvature has been represented as a population of geometrically necessary dislocations (GNDs). When the density of GNDs becomes sufficiently large, their redistribution produces subgrains, which can be treated as the above mentioned two phase cell model.

An alternative model of HPT ultra-fine substructure development has been suggested in [12]. The proposed crystal plasticity model has been inspired by systematic parameter studies of the microstructure evolution with increasing strain in copper, nickel and Armco iron deformed by conventional and cyclic HPT reported in [13-15]. The experiments were directed towards exploring the basic questions: the way of fragmentation of the original grains into much smaller structural elements, the question of the existence of a saturation in the structural refinement, and how temperature, pressure and cycling affect these phenomena. The results of these measurements provide a base for theoretical analysis and modelling of the fragmentation process. In the present paper, the evolution of the HPT microstructure is considered in a volume element shown in Fig. 1.

In [13,14], the microstructure was observed in sections perpendicular to the radial direction (z-axis) and to the axial direction (y-axis). The observations provide detailed data on the shapes and preferred alignment of the structural elements, their misorientation, size and texture. They can be summarized as follows:

- The observations excluded grain boundary sliding as the main mechanism in explored HPT;

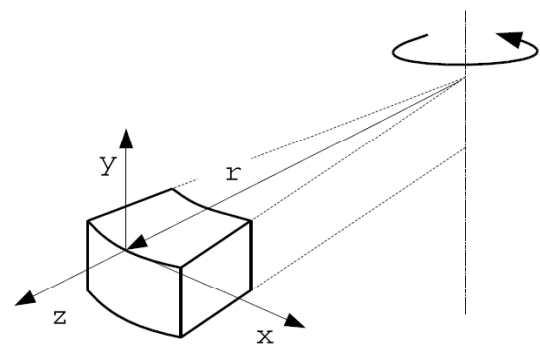


Fig. 1. The volume element.

the conclusion reported in [15] that the HPT shearing imposed by torsion was achieved by intergranular glide has been accepted as a principle guideline of our theoretical study.

- Preferred alignment of structural elements observed in radial direction is inclined with respect to the torsion axis; the alignment is changing with reverse of twist; no alignment is observed in axial direction.
- Misorientation between structural elements (grains, subgrains, cells) increases with strain; the elements are separated by layers called “non-equilibrium boundaries”.
- The size of structural elements decreases with increasing strain and reaches a steady state.
- The steady state saturation is observed after strain ~ 20 ; no further structural refinement occurs and no further work hardening is observed. A characteristic feature observed in the saturated state is a pronounced shear texture.
- The study [15] revealed that single crystals with different crystallographic orientation and polycrystals develop in saturation a similar microstructure and microtexture.

Accepting the observation that HPT shearing is achieved by intergranular glide the fragmentation process is interpreted within the framework of crystal plasticity. In Section 2 the considerations are restricted to rigid-plastic deformation carried by an effective double slip. In the present context the term “effective” is used as a convenient substitute of a correlated activity of several slip systems in plane strain conditions. This approach was proposed and experimentally tested by Harren *et al.* [16]; their model is briefly summarized in Section 2.

The assumption of the plane-strain double-slip does not cover the fragmentation as seen in the axial

direction. The most distinguished feature related to the axial fragmented pattern is the gradient of plastic strain in the radial direction. In the plane-strain approximation the geometrical necessary dislocations (GND) forming structural element boundaries seen in the radial direction have an edge character. From this point of view, GNDs in the axial direction could be modelled as screw parts connecting the edge segments to form dislocation loops. Therefore the main concern presented in the following sections is the analysis directed to an evolution of the radial pattern.

The idealized framework provides a possible qualitative explanation of some of the observations summarized above. The basic feature of the model is a rotation of the slip systems carrying the imposed HPT strain. The slip activity is governed by the shear stress imposed by torsion and by axial compression. The analysis of the lattice rotation and the stress evolution serves as a basis for application of the model of misoriented structure formation [17] to HPT. There the spontaneously formed misoriented cells arise due to intersection of two shear band systems. The model is a realization of the belief noted by Rosochowski [18]: “The mechanism responsible for this effect (creation of submicrometer sized subgrains) is still under investigation, however, it is believed that short and long intersecting shear bands produced by plastic deformation play a major role”. In Section 3 it is suggested, that the formation of the misoriented structural elements can be interpreted as an instability of homogeneous shearing. The effective rotation of the slip systems causes a continuous reconstruction of the pattern. It seems that this effect leads to an increase in the dislocation density and to an enhanced hardening.

2. THE CRYSTAL PLASTICITY MODEL

In the proposed continuum mechanics model the HPT deformation is interpreted as a plastic flow through the adjustable crystal lattice. In the rigid-plastic approximation adopted the distortion of the lattice is reduced to a lattice rotation. The model is described by the Cauchy stress $T(x, t)$, by the velocity field $u(x, t)$, and by three scalar internal variables: the orientation of the crystal lattice $\alpha(x, t)$ and critical yield stresses $\tau_y^{(i)}(x, t)$, $i = 1, 2$. We use the Eulerian description: x is a position at the current configuration and t means time. The fields T and u have to satisfy the following set of conditions:

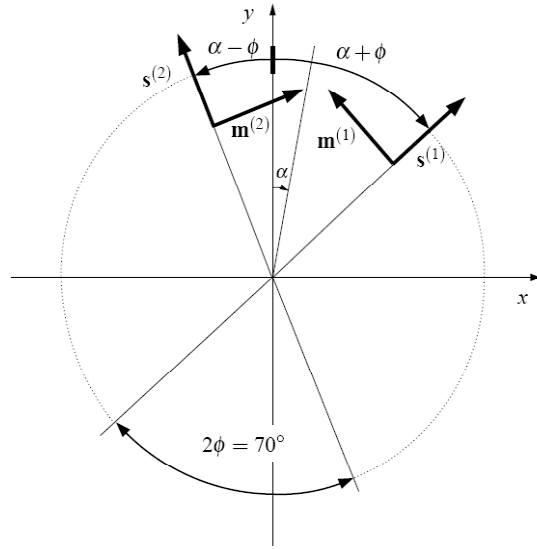


Fig 2. Slip systems - double slip.

incompressibility

$$\operatorname{div} u = 0, \quad (1)$$

equilibrium

$$\operatorname{div} T = \operatorname{div} S - \nabla p = 0, \quad (2)$$

dissipation rate

$$T \cdot D \geq 0, \quad (3)$$

where the stress T is decomposed into its spherical part $-pI$, p is the pressure, and the deviatoric part S , i.e. $T = -pI + S$, and $D = 1/2(\nabla u + (\nabla u)^T)$. The velocity gradient $L = \nabla u$ consists of plastic flow gradient L^p and the rate of distortion of the crystal lattice represented by the lattice spin $L^e = \dot{R}^e (R^e)^T$, where $R^e(x, t)$ is a lattice rotation; a superposed dot means differentiation with respect to time t .

The plastic flow takes place on prescribed slip systems (i) , $i = 1, 2, \dots, I$. The (i) slip system is defined by the unit vector $s^{(i)}$ in the direction of slip and by the unit normal to the glide plane $m^{(i)}$. In the rigid-plastic approximation the vectors $s^{(i)}$ and $m^{(i)}$ rigidly rotate with the lattice. The plastic flow is governed by slip rates $v^{(i)}(x, t)$ on the individual slip systems via the flow rule

$$L^p = \sum_{i=1}^I v^{(i)} s^{(i)} \otimes m^{(i)}. \quad (4)$$

In summary, kinematics of the rigid-plastic flow model is governed by the equation:

$$\nabla u = L = \dot{R}^e (R^e)^T + \sum_{i=1}^I v^{(i)} s^{(i)} \otimes m^{(i)}. \quad (5)$$

As indicated in Introduction the fragmentation process seen in the radial direction of HPT test can be treated as plane-strain effective double slip. There are the following reasons to accept this assumption. First, an activity of two slip systems is sufficient to carry any plane strain isochoric deformation. Second, there is a tendency to reduce the number of active slip system to avoid energetically costly multislip (single slip is not able to carry the strain imposed by HPT, unless it is parallel to the imposed shear). However, the double slip assumption has been mainly inspired by the detailed study (experimental and computational) of structure and micromechanisms of strain localization process during plane strain compression (PSC) of fcc single crystals and polycrystals in a channel die performed by Harren *et al.* [16]. X-ray measurements were carried out to determine the lattice reorientation of the single crystals of various initial crystallographic orientations. It was observed that except for crystals oriented symmetrically with respect to the compression and extension axes, the crystals exhibited an overall common behavior. After yield, all these crystals started to reorient in such a way that the resulting deformation has been aligned with the channel; the state of plane strain crystallographic deformation is approached. In order to simulate the compression tests of single crystals, Harren *et al.* [16] employed a two-dimensional single crystal model with the two effective slip systems. The experimental observations and the computed deformation response were in a close agreement. In the PSC tests of polycrystals [16], the observed micromechanics demonstrated that highly nonuniform grain deformations and lattice rotations provided a 'crystallographic path' that allowed slip to be transmitted across grain boundaries. The FEM calculations based on a plane strain model of the polycrystal have been consistent with the experimental observations. The study revealed that in the early stages of deformation the grains tend to rotate toward an ideal texture orientation.

Inspired by this successful model we use a crystallographic double slip plane strain approximation for the analysis of the slip systems behavior in HPT. In plane strain the deformation process depends only on the coordinates x, y in the strained plane, i.e. $L(x, y, t)$, $R^e(x, y, t)$ and $L^p(x, y, t)$.

Let the slip directions $s^{(i)}$ and the normals $m^{(i)}$, $i = 1, 2$, in the current configuration be

$$\begin{aligned} s^{(1)} &= (\sin(\alpha + \phi), \cos(\alpha + \phi)), \\ s^{(2)} &= (\sin(\alpha - \phi), \cos(\alpha - \phi)), \\ m^{(1)} &= (-\cos(\alpha + \phi), \sin(\alpha + \phi)), \\ m^{(2)} &= (\cos(\alpha - \phi), -\sin(\alpha - \phi)). \end{aligned} \quad (6)$$

$\alpha(x, y, t) + \phi$ and $\alpha(x, y, t) - \phi$ are the angles of the slip directions $s^{(1)}$, $s^{(2)}$ with respect to the compression axis y , α is angle of the symmetry axis between slip directions, and ϕ a fixed angle given by slip crystallography, Fig. 2. In the present case we take $\phi = 35^\circ$, which is characteristic of a plane strain approximation of f.c.c. crystals (the complementary angle $\phi = 55^\circ$ provide the same results). The internal variable $\alpha(x, y, t)$ measured in clockwise direction from the y -axis determines the local rotation of the crystal lattice R^e

$$\begin{aligned} R^e &= \begin{pmatrix} \cos \alpha & -\sin \alpha & 0 \\ \sin \alpha & \cos \alpha & 0 \\ 0 & 0 & 1 \end{pmatrix}, \\ \dot{R}^e (R^e)^T &= \begin{pmatrix} 0 & -\dot{\alpha} & 0 \\ \dot{\alpha} & 0 & 0 \\ 0 & 0 & 0 \end{pmatrix}. \end{aligned} \quad (7)$$

According to Eq. (5) the velocity gradient L consists of the contributions from the slip rates $v^{(1)}$ and $v^{(2)}$ carried by the considered two slip systems, and of the lattice spin $\dot{R}^e (R^e)^T$; in components

$$\begin{aligned} \begin{pmatrix} L_{xx} & L_{xy} \\ L_{yx} & -L_{xx} \end{pmatrix} &= \\ \frac{v^{(1)}}{2} \begin{pmatrix} -\sin 2(\alpha + \phi) & 2 \sin^2(\alpha + \phi) \\ -2 \cos^2(\alpha + \phi) & \sin 2(\alpha + \phi) \end{pmatrix} &+ \\ \frac{v^{(2)}}{2} \begin{pmatrix} \sin 2(\alpha - \phi) & -2 \sin^2(\alpha - \phi) \\ 2 \cos^2(\alpha - \phi) & -\sin 2(\alpha - \phi) \end{pmatrix} &+ \\ \begin{pmatrix} 0 & -\dot{\alpha} \\ \dot{\alpha} & 0 \end{pmatrix}, & \end{aligned} \quad (8)$$

where $L_{xx} = \partial u_x / \partial x$, $L_{xy} = \partial u_x / \partial y$, $L_{yx} = \partial u_y / \partial x$, and $L_{yy} = \partial u_y / \partial y = -L_{xx}$. From (8) we get the following kinematical equations

$$v^{(1)} = -\frac{2L_{xx} \cos 2(\alpha - \phi) - (L_{xy} + L_{yx}) \sin 2(\alpha - \phi)}{\sin 4\phi}, \quad (9)$$

$$v^{(2)} = -\frac{2L_{xx} \cos 2(\alpha + \phi) + (L_{xy} + L_{yx}) \sin 2(\alpha + \phi)}{\sin 4\phi}. \quad (10)$$

and the evolution equation for the internal variable α ;

$$\dot{\alpha} = \frac{-L_{xx} \sin 2\alpha - L_{xy} \cos(\alpha + \phi) \cos(\alpha - \phi) + L_{yx} \sin(\alpha + \phi) \sin(\alpha - \phi)}{\cos 2\phi}. \quad (11)$$

The stress T controls the rates $v^{(i)}(x, t)$ through the resolved shear stresses $\tau^{(i)}(x, t)$

$$\tau^{(i)} = s^{(i)} \cdot Tm^{(i)}, \quad (12)$$

from (6) and (12)

$$\begin{aligned} \tau^{(1)} &= -S_{xx} \sin 2(\alpha + \phi) - S_{xy} \cos 2(\alpha + \phi), \\ \tau^{(2)} &= S_{xx} \sin 2(\alpha - \phi) + S_{xy} \cos 2(\alpha - \phi). \end{aligned} \quad (13)$$

where $S_{xx} = (T_{xx} - T_{yy})/2$ and $S_{xy} = T_{xy}$.

Two constitutive versions of the model can be considered: the rigid-viscous-plastic (rate dependent), the rigid-plastic (rate independent)

1. In rigid-viscous-plastic version the resolved shear stresses $\tau^{(1)}$ and $\tau^{(2)}$ are coupled with the slip rates $v^{(1)}$ and $v^{(2)}$ through a power law constitutive equation (viscoplastic yield condition)

$$\tau^{(i)} = \tau_y^{(i)} |v^{(i)}|^q \text{sign } v^{(i)}, \quad (14)$$

where $q > 0$ is a scalar material parameter, which controls the rate sensitivity and $\tau_y^{(i)}(x, y, t)$, $i = 1, 2$, are the internal variables called critical resolved shear stresses.

2. In rigid-plastic version the slip rates $v^{(1)}$ and $v^{(2)}$ are governed by the yield condition: slip system remains active, i.e. $v^{(i)}$ may be non-zero, if and only if

$$\tau^{(i)} = \tau_y^{(i)} \text{sign } v^{(i)}. \quad (15)$$

This version can be understood as a limit of the version 1 for the rate sensitivity exponent $q \rightarrow 0$.

In both versions the critical resolved shear stresses $\tau_y^{(i)}(x, y, t)$, $i = 1, 2$, are governed by evolution equation, $i = 1, 2$,

$$\dot{\tau}_y^{(i)} = \sum_{j=1}^2 H_{ij} |v^{(j)}|. \quad (16)$$

The hardening matrix components H_{ij} are taken as given material parameters.

3. LATTICE ROTATIONS

The rotation of the slip systems rigidly connected with the crystal lattice was studied in [12]. There was assumed that the considered volume element is a part of single crystal deformed in double slip. A uniform deformation was analyzed, i.e. the field variables of crystal plasticity introduced in Section 2 are spatially homogeneous and depend on time t only. In the uniform plane-strain simplification of the HPT, the volume element is subjected to simple shear. The corresponding velocity gradient $L(t)$ is

$$L = \begin{pmatrix} 0 & L_{xy} \\ 0 & 0 \end{pmatrix}, \quad (17)$$

where $L_{xy}(t)$ is determined by the imposed torsion. The shear flow rate L_{xy} can be defined approximately as $L_{xy} \approx r \dot{\theta}/h$, where $\theta(t)$ is the twist angle, h is the height of the cylindrical specimen and r is the distance from the torsion axis, cf. Introduction, Fig. 1.

Eqs. (9-11) with L in the form (17) are reduced to:

$$\begin{aligned} v^{(1)} &= \frac{L_{xy} \sin 2(\alpha - \phi)}{\sin 4\phi}, \\ v^{(2)} &= -\frac{L_{xy} \sin 2(\alpha + \phi)}{\sin 4\phi}. \end{aligned} \quad (18)$$

and the evolution equation for the internal variable α is:

$$\dot{\alpha} = -\frac{L_{xy} \cos(\alpha + \phi) \cos(\alpha - \phi)}{\cos 2\phi}. \quad (19)$$

From these equations it was deduced, cf. [12], that for any initial lattice orientation the double slip develops towards single slip, i.e. either $v^{(1)}$ or $v^{(2)}$ finally vanishes. The single slip regimes, once reached, could persist. This means, if there is a disturbance of the single slip regime, the lattice spin acts against the disturbance, thus returning the crystal orientation to the single slip one. However, to reach the stable single slip, an infinite deformation is needed, i.e. the shear component of the deformation gradient $F_{xy} \rightarrow \infty$. The reason is that in the considered case of simple shear of the volume element, we get for deformation gradient F from $\dot{F} = LF$ that $\dot{F}_{xy} = L_{xy}$ and from (19),

$$\dot{\alpha} = -\frac{\dot{F}_{xy} \cos(\alpha + \phi) \cos(\alpha - \phi)}{\cos 2\phi}. \quad (20)$$

The singularity of F_{xy} is revealed by integration of Eq. (20). Thus the single slip orientation in a volume element deformed in plane-strain simple-shear in double slip is reached asymptotically. The detailed analysis is given in [12].

In HPT experiments, an axial torque is combined with a high axial compression. Under these loading conditions, the sample is exposed to a shear stress, to an axial compression, and to a hydrostatic pressure. The shear stress is induced by the applied

torque. The stress in the sample imposed by the applied axial compression of the HPT tool can be divided into the axial compression stress and the hydrostatic pressure. The reason for the partition is that up to the current flow stress, the tested material of the specimen together with the HPT tool behave as a body consisting of two elastic parts in contact exposed to a compression. Only the part of the stress in the sample stemming from the applied compression which exceeds the current flow stress acquires a hydrostatic character, because the material of the sample flows. FEM simulations of the HPT experiments [19] confirmed such stress field interpretation.

4. FRAGMENTATION

Conventional explanations of a fragmentation process in a form of subgrains or misoriented dislocation cell formation use either statistical argument [20] or assume a preexisting structure of obstacles in the crystal [21,22]. According to an alternative approach, dislocations are forced by the laws of non-linear continuum mechanics to arrange themselves into periodic patterns of varying density. From this point of view, the inhomogeneity of plastic deformation is the basic reason for subgrain formation. Plastic deformation and rotation of different volume elements proceed in an organized way so that the long-range internal stresses which would be set up by deformation of a single volume element are reduced by deformation and rotation of neighboring volume elements [23-25]. The reason for the plastic deformation being non-homogeneous is a possible instability of homogeneous plastic flow. In addition to the macroscopic instabilities of plastic deformation in the form of necking or shear band formation, there is an instability in the form of internal buckling [26-28]. This instability is made possible by the inherent anisotropy of plastic deformation. Under certain circumstances, more strain energy is available in the uniform plastic deformation than is required to initiate an internal mode of buckling. In such a case, the internal instability makes its appearance. It has been suggested to interpret the internal instability of homogeneous plastic flow in terms of the formation of misoriented dislocation cells or subgrains [17,29-31]. It has been shown that the internal buckling leads to the build up of lattice misorientations between neighboring volume elements. The periodic patterns of dislocations necessary to accommodate the lattice misorientations were interpreted as the beginning of subgrain formation. It should be pointed out, however, that the approach itself - which is es-

essentially an application of the classical continuum crystal plasticity [32-35] completed by the theory of geometrically necessary dislocations [36,37] - is in principle applicable to plastic deformation in general [17,31,38-41].

In the present paper the above mentioned approach provides a qualitative explanation of some features of the fragmentation process as observed in HPT experiments [13-15]. Within the proposed framework the fragmentation is treated as spontaneous structuralization of an instability character. In solution of this problem we might encounter complexity and difficulties akin to the problem of turbulence. Nevertheless, valuable information on initial stages and trends in fragmentation can be obtained from stability analysis of the model. The analysis is rather complex and it will be presented in detail in a subsequent publication. Here, some preliminary results are briefly summarized.

In the linear stability analysis all quantities describing a homogeneous flow (denoted by bar $\bar{}$) are perturbed by introducing "infinitesimal" disturbances of the shape of a plane wave (denoted by hat $\hat{}$). To illustrate that, let \bar{s} be one of the quantities describing the basic flow (velocity u , velocity gradient L , slip rates $v^{(1)}$ and $v^{(2)}$, rotation angle α , deviatoric stress S , pressure p , and critical resolved shear stresses $\tau_y^{(1)}$ and $\tau_y^{(2)}$). After perturbation

$$s = \bar{s} + \hat{s}, \quad (21)$$

where

$$\hat{s} = \tilde{s} \exp(ik_x x + ik_y y + \omega t) \quad (22)$$

is the wave-like disturbance expressed in a convenient complex form. The wave can be understood as a Fourier component of a general infinitesimal perturbation. Here \tilde{s} is a real amplitude, (k_x, k_y) are components of wave vector, and ω is an attenuation factor of the disturbance. The growth or decay of disturbance (22) is fully determined by the real part of ω . The wave with the maximum positive ω indicates a dominant instability mode.

Introducing the field variables in the form (21), (22) into the model described in Section 2 one gets a system of linearized algebraic equations for amplitudes: $\tilde{u}_x, \tilde{u}_y, \tilde{v}^{(1)}, \tilde{v}^{(2)}, \tilde{\alpha}, \tilde{S}_{xx}, \tilde{S}_{xy}, \tilde{p}, \tilde{\tau}_y^{(1)}$, and $\tilde{\tau}_y^{(2)}$. If A denotes the matrix of the system, the condition of solubility $\det A(\omega, k_x, k_y) = 0$ provides the relation between the attenuation factor ω and the wave vector (k_x, k_y) . For the rate independent version of the model (15) and the symmetric hardening matrix: $H = H_{11}/\bar{\tau} = H_{22}/\bar{\tau}, Q = H_{12}/\bar{\tau} = H_{21}/\bar{\tau}$, where $\bar{\tau} = \bar{\tau}_y^{(1)} = \bar{\tau}_y^{(2)}$ is the initial value of the resolved shear

stresses, the dependence $\omega(k_x, k_y)$ can be expressed in the form

$$\bar{\omega}(\xi) = \frac{4Ha_H(\xi, \alpha, \phi) + Q \sin 2\alpha a_o(\xi, \alpha, \phi)}{H \sin 4\phi b_H(\xi, \phi) + Qb_o(\xi, \phi)}, \quad (23)$$

where

$$\begin{aligned} a_H &= \xi \cos(2\alpha + \phi)(\xi \cos \phi + \sin \phi)^2 (\xi \sin \phi - \cos \phi) - \\ &\xi \cos(2\alpha - \phi)(\xi \cos \phi - \sin \phi)^2 (\xi \sin \phi + \cos \phi) + \\ &\sin(2\alpha - \phi)(\xi \cos \phi - \sin \phi)^2 (\xi \sin \phi + \cos \phi) - \\ &\sin(2\alpha + \phi)(\xi \cos \phi + \sin \phi)^2 (\xi \sin \phi - \cos \phi), \\ a_o &= [1 - \xi^2 - (1 + \xi^2) \cos 2\phi] \times \\ &[2\xi(\cos(\alpha - \phi) + \cos(\alpha + \phi)) - \\ &2(1 + \xi^2 + (1 + \xi^2) \cos 2\phi)], \end{aligned}$$

$$\begin{aligned} b_H &= 1 + 2\xi^2 + \xi^4 - (1 - 6\xi^2 + \xi^4) \cos 2\phi + \\ &2(1 - \xi^2)[1 - \xi^2 - (1 + \xi^2) \cos 2\phi], \\ b_o &= -1 + 6\xi^2 - \xi^4 + (1 + \xi^2)^2 \cos 4\phi, \end{aligned}$$

$$\bar{\omega} = \frac{\omega}{L_{xy}}, \text{ and}$$

$$\xi = \frac{\zeta \cos \bar{\alpha} + \sin \bar{\alpha}}{-\zeta \sin \bar{\alpha} + \cos \bar{\alpha}},$$

$$\zeta = \frac{k_x}{k_y}.$$

The attenuation factor $\bar{\omega}$ indicates strong instabilities. They occur for the ratio ξ equal to the roots of the denominator of (23). The instabilities represented by singularities of $\bar{\omega}(\xi)$ are shown in Fig. 3 for $\phi = 35^\circ, H = 100, Q = 140$. For these values the roots are: $\xi = \pm 2.25$ and $\xi = \pm 0.45$. From the analysis of the perturbed equations it follows that the singularities in the instability spectrum (23) result from the fact that HPT forces the slip systems to rotate, cf. (11) and Section 3. The singular character itself seems to be a consequence of the introduced simplifying assumptions: rate independence and elastic rigidity. Both viscosity in rate dependent version of the model and elastic strain would have a smoothing effect. However, the stability analysis in the latter case is more complicated.

The scheme of the corresponding fragmented pattern is outlined in Fig. 4 for $\xi = \pm 2.25$. The frag-

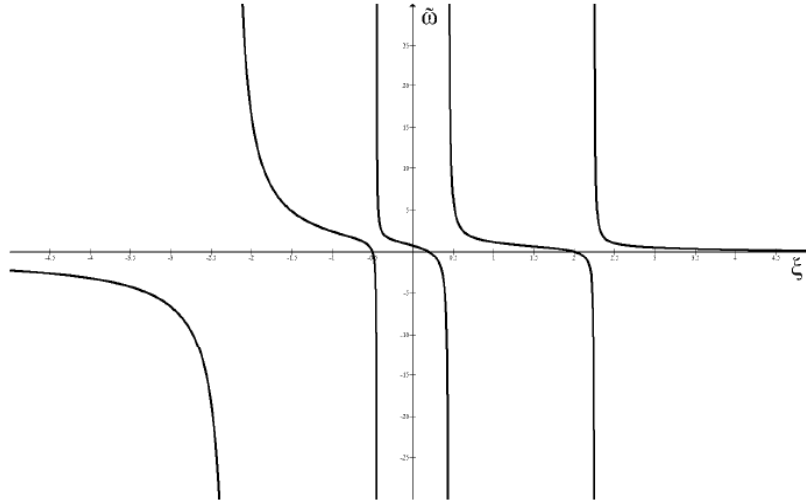


Fig. 3. The instability spectrum, see Eq. (23).

mentation is represented by two crossing lamellar substructures (shear bands) symmetrically oriented with respect to the crystal orientation subjected to rotation as shown in Section 3.

The double slip activity in the lamellar substructures is controlled by the instability slip rates, $i = 1, 2$:

$$\hat{v}^{(i)} = \tilde{v}^{(i)} \exp(\omega t)$$

$$\sin \left\{ \frac{k}{\sqrt{1 + \xi^2}} \right. \quad (24)$$

$$\left. [(\xi \sin \bar{\alpha} + \cos \bar{\alpha})x + (\xi \sin \bar{\alpha} - \cos \bar{\alpha})y] \right\},$$

where

$$\zeta = \frac{k_x}{k_y} = \frac{\xi \sin \bar{\alpha} + \cos \bar{\alpha}}{\xi \sin \bar{\alpha} - \cos \bar{\alpha}}$$

determines the orientation of the pattern which rotates with $\bar{\alpha}$, k is the magnitude of the wave vector, and the ratio between the instability amplitudes is

$$\frac{\tilde{v}^{(1)}}{\tilde{v}^{(2)}} = - \frac{(\xi^2 - 1) \sin 2\phi + 2\xi \cos 2\phi}{(\xi^2 - 1) \sin 2\phi - 2\xi \cos 2\phi}. \quad (25)$$

In the considered example $\phi = 35^\circ, H = 100, Q = 140, \xi = \pm 2.25$ the ratio $\frac{\tilde{v}^{(1)}}{\tilde{v}^{(2)}} = 2.35$. In Fig. 4 the relative slip activity in the fragmented structural elements

is schematically depicted by the density of the slip lines. The symbols of geometrically necessary dislocations indicate the rate of the misorientation between neighboring structural elements (the misorientation itself is not shown). An analogical pattern can be drawn for $\xi = \pm 0.45$. It is not clear yet, which of these fragmented patterns would dominate or if a combination of both prevails. This problem requires further, namely energetic analysis.

The wave length of the pattern $\lambda = 2\pi/k$ is not specified by the model as the instability spectrum

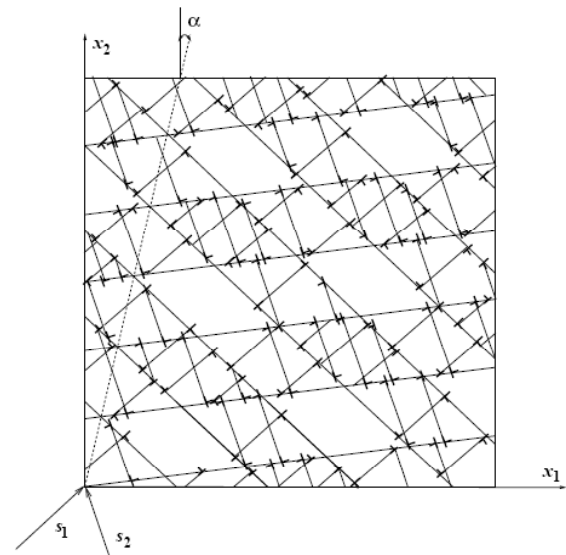


Fig. 4. Scheme of misoriented fragmented structural elements.

$\omega(\zeta)$ depends just on $\zeta = k_x/k_y$. As already noted by Biot [28], the standard continuum mechanics which contains no length scale predicts the zero cell size as it leads to the lowest energy. However, the mutually misoriented structural elements fit together by means of geometrically necessary dislocations forming the fragment boundaries. To form the boundaries, an interface energy is needed. When the fragment size decreases, the number of fragment elements per unit volume, the interface area, and the related interface energy increase. From this point of view, the fragment size is a compromise between these two energetically driven tendencies. An approximate formula for the fragment size has been derived in [17] and adopted to HPT in [12]. Let us recall that the plane-strain model of symmetric double slip of a crystal in tension [17] has incorporated the non-local effect caused by close range dislocation interactions. It has provided an order of magnitude estimate of the cell size expressed by the factor R (Eq. (75) in [17]),

$$R \approx \frac{GD}{\kappa\rho\delta}, \quad (26)$$

where G is the shear modulus, D the non-local hardening parameter deduced from dislocation statistics to be of order $D \approx 1$, κ represents the local hardening expressed in the present model by the hardening coefficients H_{ij} , ρ is the total density of dislocations in the cell boundaries, and δ is the width of the boundaries. The order of magnitude estimate of R for values characteristic of metal crystals in tension: $G = 3 \times 10^{10}$ Pa, $h \approx 10^8$ Pa, $\delta \approx 10^{-9}$ m, and $10^{15} \text{ m}^{-2} < \rho < 10^{17} \text{ m}^{-2}$. Then R is in the range $3 \mu\text{m} < R < 300 \mu\text{m}$. If we employ for an estimate of the structural size in HPT the same approach, we can expect no change in G and D , as both are of elastic nature. On the other hand, the observed non-equilibrium boundaries are wider than $\delta \approx 10^{-9}$ m of standard grain boundaries. The rotation of the slip system may have a similar effect as a change of loading trajectories (e.g. in [42], it was demonstrated that the stress is the highest for a 'circular' continuous change of loading trajectories). Changes in deformation microstructure caused by simple shear in steel pre-deformed in tension were studied in [43]. It was observed that the new dislocation cells correlated to the subsequent loading gradually replace the cell structure caused by the pre-strain. Dislocation structures resulting from tension vanish when the shear strain exceeds the pre-strain amount. In HPT, the rotation of the slip systems may cause a

continuous replacement. It might be that non-equilibrium boundaries are less suitable as annihilation centers thus increasing hardening and the dislocation density. Therefore, there is a reason to suppose that the denominator in (26) for HPT is significantly higher than in conventional tests, hence, the structural size becomes smaller.

5. DISCUSSION

The proposed crystal plasticity model analyzed in the previous sections has revealed three essential features of the HPT deformation:

- (i) To satisfy the imposed HPT loading conditions, the slip systems have to rotate and change their activities during the deformation process. This feature has been treated as effective rotation of the double slip.
- (ii) The rotation approaches the single slip orientation of simple shear which provides a base for the steady state saturation.
- (iii) The fragmentation of structural elements has been interpreted as a spontaneous structuralization assisted by effective rotation of the slip systems.

Despite of the introduced simplifications (rigid-plastic, rate independent, plane strain approach) the results of stability analysis of the model provides valuable information. It reveals the initiation of the fragmentation process and trends of its evolution. Based on these conclusions we try to interpret some of the observed features in the HPT experiments as itemized in Introduction.

- If one accepts that the HPT shearing imposed by torsion was achieved by intergranular glide, the proposed mechanism of the spontaneous HPT substructure formation is a direct consequence of crystal plasticity theory. Moreover, one of the main features of HPT, a changing of a strain trajectory treated in the presented model as the effective rotation of the slip systems, occurs also in other severe plastic deformation processing techniques, typically in equal-channel angular pressing. Therefore, it seem possible that there the mechanism of formation of the ultra-fine grain substructure could be of similar crystal plasticity origin.
- The tendency of the fragment pattern to follow the orientation of the slip systems demonstrated in Fig. 4 might be a reason for the observed preferred alignment of the structural elements inclined with respect to the torsion axis [13]. The hypothesis is supported by the results of the cyclic HPT [14] where the direction of the pre-

ferred alignment is changing with the reverse of twist. The proposed model exhibits a similar feature: the reverse of the applied shear rotates the slip systems in the opposite direction and the newly formed pattern would tend to form a mirror preferred alignment.

- The model predicts that the misorientation increases with strain, as seen in (24); the perturbations exhibit exponential growth. However, unlike the observed tendency to a randomly distributed large misorientations [13], the modelled misorientations are small periodic deviations from the uniform orientation. From the proposed HPT model, one can deduce that the boundaries between adjacent structural elements may have a special structure different from the standard grain boundaries. At each orientation of the slip systems, there is a tendency to build a particular pattern. Due to the rotation of the systems, these patterns may overlap. This might be a reason for formation of the observed dislocation layers of finite thickness separating the structural elements, the so called 'non-equilibrium boundaries'. According to this hypothesis, the boundaries formed in later stages of deformation, where the rate of rotation per applied shear strain diminishes, should be better defined and be akin to the 'true' grain boundaries.
- A rough estimate of the fragment size is given by (26). It must be emphasized, however, that the estimate does predict neither the observed evolution nor the saturation of the pattern size. Moreover, the formula (26) incorporates the non-local effects caused by close range dislocation interactions, which are not yet included in the version of the model presented in Section 2.
- Within the framework of the proposed model, the saturation is related to the states of stable orientation, $\bar{\alpha} = \pm 90^\circ$, where for any initial lattice orientation the double slip develops towards single slip. The single slip regimes, once reached, could persist. However, a saturated steady state needs to build a microstructure, where generation and annihilation of dislocations are in equilibrium. A matured fragmented substructure of saturated state should provide a sufficient density of effective generation-annihilation centers either within the fragment boundaries or to build additional accidental annihilation centers.
- The observations [15] that single crystals with different crystallographic orientation and polycrystals develop in saturation a similar microstruc-

ture and microtexture can be related to the results of FEM calculation by Harren *et al.* [16] recalled in Section 2: the shearing within a single grain often behaves in a similar manner to that within the single crystals. Perhaps in future, the presented HPT model will predict analogous features.

ACKNOWLEDGEMENTS

Thanks are due to our former student A. Warzynski for help with algebraic calculations. The research has been supported by the grants VZ-MSMT 6840770003 (J.K.), VZMSMT 6840770021, and P201/10/0357 (GACR).

REFERENCES

- [1] R.Z. Valiev and T.G. Langdon // *Review on Advance Materials Science* **13** (2006) 15.
- [2] T.G. Langdon // *Review on Advance Materials Science* **13** (2006) 6.
- [3] R.Z. Valiev and T.G. Langdon // *Progress in Materials Science* **51** (2006) 881.
- [4] A.P. Zhilyaev and T.G. Langdon // *Progress in Materials Science* **53** (2008) 893.
- [5] F.A. Mohamed // *Acta Materialia* **51** (2003) 4107.
- [6] Y.H. Zhao, Y.T. Zhu, X.Z. Liao, Z. Horita and T.G. Langdon // *Materials Science and Engineering A* **463** (2007) 22.
- [7] L. Tóth, A. Molinari and Y. Estrin // *J. Engineering Materials and Technology* **124** (2002) 71.
- [8] P.W.J. McKenzie, R. Lapovok and Y. Estrin // *Acta Materialia* **55** (2007) 2985.
- [9] I.V. Alexandrov and R.G. Chembarisova // *Review of Advance Materials Science* **16** (2007) 51.
- [10] Y. Estrin, A. Molotnikov, C.H.J. Davies and R. Lapovok // *J. Mechanics and Physics of Solids* **56** (2008) 1186.
- [11] L. Tóth, Y. Estrin and R. Lapovok, In: *Congress on nanotechnologies: 2nd Int. Symposium on bulk nanostructured materials*, ed. by R.Z. Valiev (BNM 2009, Ufa, Russia), p. 162.
- [12] J. Kratochvíl, M. Kružík and R. Sedláček // *Acta Materialia* **57** (2009) 739.
- [13] T. Hebesberger, H.P. Stüwe, A. Vorhauer, F. Wetscher and R. Pippan // *Acta Materialia* **53** (2005) 393.
- [14] F. Wetscher and R. Pippan // *Philosophical Magazine* **86** (2006) 5867.

- [15] M. Hafok and R. Pippan // *Scripta Materialia* **56** (2007) 757.
- [16] S.V. Harren, H.E. Dève and R.J. Asaro // *Acta Metallurgica* **36** (1988) 2435.
- [17] J. Kratochvíl, M. Kružík and R. Sedláček // *Physical Review B* **75** (2007) 4104.
- [18] A. Rosochowski // *Solid State Phenomena* **101-102** (2005) 13.
- [19] W. Ecker, *Master's thesis* (Montanuniversität Leoben, A-8700 Leoben, Austria, March 2004).
- [20] D. Kuhlmann-Wilsdorf and N. Hansen // *Scripta Metallurgica et Materialia* **25** (1991) 1557.
- [21] A. Orlová and J. Čadek // *Philosophical Magazine* **21** (1970) 509.
- [22] T. Hasegawa, U.F. Kocks and R.O. Scattergood // *Scripta metallurgica* **14** (1980) 449.
- [23] W. Blum, In: *Plastic Deformation and Fracture of Materials*, ed. by H. Mughrabi. chapter 8 (VCH Verlagsgesellschaft, Weinheim, 1993), p. 359.
- [24] W. Blum and H. J. McQueen // *Materials Science Forum* **217-222** (1996).
- [25] W. Blum, In: *The Johannes Weertman Symposium*, ed. by R. W. Arsenault, D. Cole, T. Gross, G. Kostorz, P. Liaw, S. Parameswaran, H. Sizek (1996), p. 103.
- [26] M.A. Biot // *Proceedings Royal Society A* **273** (1963) 306.
- [27] M.A. Biot // *Journal of the Franklin Institute* **279** (1965) 65.
- [28] M. A. Biot, *Mechanics of Incremental Deformations* (JohnWiley, New York, 1965).
- [29] J. Kratochvíl // *Scripta Metallurgica et Materialia* **24** (1990) 1225.
- [30] J. Kratochvíl and A. Orlová // *Philosophical Magazine A* **61** (1990) 281.
- [31] J. Kratochvíl and R. Sedláček // *Physical Review B* **67** (2003) 094105.
- [32] J.R. Rice // *J. Mech. Phys. Solids* **19** (1971) 433.
- [33] R. Hill and J.R. Rice // *J. Mech. Phys. Solids* **20** (1972) 401.
- [34] J.R. Rice, In: *Constitutive Equations in Plasticity*, ed. by A.S. Argon (MIT Press, Boston, 1975), p. 23.
- [35] R.J. Asaro and J.R. Rice // *J. Mech. Phys. Solids* **25** (1977) 309.
- [36] J.F. Nye // *Acta Metallurgica* **1** (1953) 153.
- [37] M. F. Ashby // *Philosophical Magazine* **21** (1970) 399.
- [38] J. Kratochvíl // *Journal of the Mechanical Behavior of Materials* **4** (1993) 235.
- [39] J. Kratochvíl // *Materials Science and Engineering A* **164** (1993) 15.
- [40] J. Kratochvíl // *Solid State Phenomena* **35-36** (1994) 71.
- [41] J. Kratochvíl and M. Saxlová // *Eur. J. Mech. A/Solids* **13** (1994) 79.
- [42] E. Tanaka, S. Murakami and M. Ooka // *J. Mech. Phys. Solids* **33** (1985) 559.
- [43] E.F. Rauch and J.-H. Schmitt // *Materials Science and Engineering A* **113** (1989) 441.